Macedonian Journal of Chemistry and Chemical Engineering, Vol. **44**, No. 1, pp. xx–xx (2025)

MJCCA9 –

ISSN 1857-5552
e-ISSN 1857-5625

Received: April 9, 2025
Accepted: April 21, 2025

DOI: 10.20450/mjcce.2025.3129
Original scientific paper

IRREVERSIBLE INACTIVATION OF THE INITIAL REDOX FORM IN SURFACE ELECTRODE MECHANISM: THEORETICAL ASPECTS IN SQUARE-WAVE VOLTAMMETRY

Pavle Apostoloski, Rubin Gulaboski*

Faculty of Medical Sciences, "Goce Delčev" University Štip, 2000 Štip, Republic of N. Macedonia
rubin.gulaboski@ugd.edu.mk

Various redox species frequently undergo irreversible inactivation under specific chemical conditions. This study explores square-wave voltammetry to examine the electrochemical behavior of lipophilic redox systems classified within the family of surface electrode mechanisms. The theoretical analysis considers an initial redox form that simultaneously undergoes an electrochemical transformation and an irreversible chemical inactivation reaction. The study presents a detailed tabulation of distinctive voltammetric patterns, assisting readers to accurately identify this electrode mechanism and distinguish it from the film loss in the square-wave voltammetry of surface-confined redox systems. The extensive collection of simulated voltammograms in this work offers insight into establishing diagnostic criteria for recognizing this mechanism. Additionally, several suitable approaches for determining the kinetics of the dual processes involved in the electrochemical mechanism are proposed. These findings are expected to help experimentalists studying metal and alloy inactivation, as well as protein-film voltammetry (PFV), to accurately characterize the considered electrode mechanism. Given the unique features of this mechanism, experimental protocols should incorporate the use of a flow-through electrochemical cell for voltammetric measurements.

Keywords: surface electrode mechanisms; metalloenzymes; protein-film voltammetry; square-wave voltammetry; graphite electrodes

ИРЕВЕРЗИБИЛНА ДЕАКТИВАЦИЈА НА ПОЧЕТНАТА РЕДОКС-ФОРМА КАЈ ПОВРШИНСКИ ЕЛЕКТРОДЕН МЕХАНИЗАМ: ТЕОРЕТСКИ АСПЕКТИ ВО УСЛОВИ НА КВАДРАТНО-БРАНОВА ВОЛТАМЕТРИЈА

Голем број супстанци често претрпуваат иреверзибилна деактивација при дефинирани хемиски услови. Во оваа студија е применета електрохемиската техника квадратно-бранова волтаметријата со цел да се испита електрохемиското однесување на липофилни редокс-системи што се класифицираат во група на површински активни редокс-системи. Во теоретскиот модел, дефинирано е сценарио во кое почетната редокс форма истовремено претрпува и електрохемиска трансформација и неповратна хемиска деактивација. Во трудот е прикажан и детален табеларен преглед со карактеристични волтаметриски одговори симулирани при различни услови. Оваа табела е од голема корист за читателите да можат прецизно да го идентификуваат овој електроден механизам, но и да го разликуваат овој електроден механизам од механизмите што се поврзани со загуба на активен редокс-филм од површината на работната електрода. Обемната колекција на симулирани волтамограми во овој труд овозможува да се дефинираат дијагностички критериуми за препознавање на овој механизам во услови на квадратно-бранова волтаметрија. Покрај тоа, во трудот се предложени и неколку теоретски протоколи што се соодветни за определување на кинетиката на двата процеса вклучени во електрохемискиот механизам. Резултатите од овој труд треба да им помогнат на експериментаторите што ги проучуваат процесите на инактивацијата на метали и легури, како и на тие што работат со протеинофилмска волтаметрија, со цел да направат прецизна карактеризација на разгледуваниот електроден механизам. Имајќи ги предвид

специфичните карактеристики на овој механизам, експерименталните протоколи треба да вклучуваат употреба на електрохемиска ќелија со проточен систем за изведување на волтаметриски мерења кај вакви системи.

Клучни зборови: површински електродни механизми; металоензими; протеинофилмска волтаметрија; квадратно-бранова волтаметрија; графитни електроди

1. INTRODUCTION

Over the past two decades, the inactivation of redox forms originating from various metal surfaces and redox enzymes has garnered considerable attention in the field of enzymology.[1] While the electrochemistry of metal surfaces provides insights into alloy activity, investigations into enzyme inactivation often yield invaluable information about the reactivity of specific groups embedded within the protein structures.

To gain a profound understanding of enzyme inactivation processes in protein-film voltammetry, it is crucial to conduct sensitive electrochemical experiments using lipophilic redox enzymes and proteins. These proteins should be strategically affixed on a specially designed working electrode made of materials that protect the redox protein from inactivation. Notably, the simplest technique for the immobilization of electrochemically active lipophilic proteins and enzymes onto diverse electrode surfaces is through the spontaneous adsorption of dissolved redox enzymes and proteins from aqueous solutions.[2–4]

Among the various electrochemical techniques that have pioneered the study of the electrochemical properties and chemical behavior of lipophilic redox proteins and enzymes, protein-film voltammetry (PFV) stands out as one of the simplest and most innovative methods introduced at the end of the last century.[2–7] In a relatively short period, the number of redox proteins and enzymes investigated through PFV has increased almost exponentially.[5–7] The appeal of PFV lies in its inherent simplicity. Using a conventional three-electrode voltammetric setup allows for the collection of pertinent data on the dynamics of various redox proteins. PFV assays typically employ only a microgram of a redox protein adsorbed onto the substrate of the working electrode, ensuring that, in most cases, the protein's functionality remains intact across successive voltammetric scans.

Numerous theoretical studies have explored different electrochemical mechanisms under PFV conditions.[8–22] However, there has been a lack of theoretical analysis of electrochemical mechanisms within square-wave voltammetry. In this study, we assume that the initial redox form of a given protein participates in both an electrochemical transition and an irreversible chemical reaction. This electrochemical mechanism is particularly significant as it frequently correlates with the deactivation pathways of various redox enzymes and proteins.[23]

This study highlights the implications of a theoretical voltammetric model examining electrode transformations of lipophilic redox proteins, where the initial redox form simultaneously undergoes an electrochemcial reaction and an irreversible chemical process. The insights presented herein aim to help experimentalists in the field of protein-film voltammetry to recognize this electrochemical paradigm and develop suitable methodologies for obtaining relevant kinetic parameters related to enzyme activity.

2. MATHEMATICAL MODEL

In the context of protein-film square-wave voltammetry, a surface-confined electrochemical mechanism is considered. It is assumed that molecules of the initial redox-active species, Ox(ads), participate in both an electrochemical transformation and a concurrent irreversible chemical reaction, as illustrated in Scheme I:

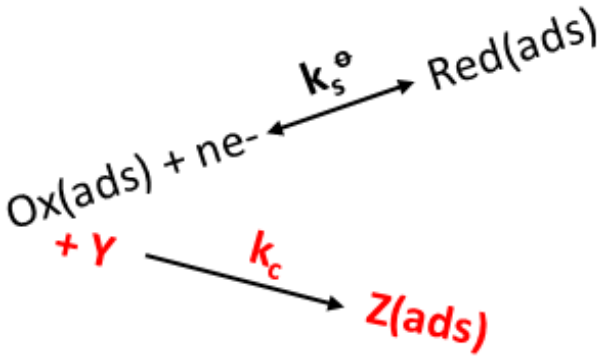

Scheme I. Schematic description of the model elaborated in this work

In the context of the mathematical model, it is assumed that molecules of the species "Ox", "Red", and "Z" are strongly adsorbed (ads) onto the working electrode surface. The model assumes no interactions among the adsorbed species and dismisses any additional mass transfer via diffu-

sion. In reaction Scheme I, the entity Y represents a substrate abundant in the electrochemical cell, which undergoes a selective irreversible chemical interaction with the electrochemically active Ox(ads) molecules. Consequently, the concentration of substrate Y remains essentially unchanged near the electrode surface throughout the voltammetric scans. This stability allows the kinetics of the irreversible chemical reaction in reaction Scheme I to be treated under pseudo-first-order conditions. Furthermore, it is presumed that the Z molecules in reaction Scheme I are electrochemically inert within the range of the applied potentials. Table 1 provides a comprehensive breakdown of the principal parameters used in the theoretical evaluations of the mechanism.

T a b l e 1

Definitions of all parameters employed in the computation of the square-wave voltammograms of the electrode mechanism elaborated in this work

Symbol of physical parameter/units	**Meaning of the parameter**	**Definition**
Ψ	Dimensionless current of simulated voltammograms	$\Psi = I/[(nFSf\Gamma^*(\mathrm{Ox})]$
I/A	Symbol of the electric current	
n	Number of electrons exchanged between working electrode and the molecules of adsorbed redox species	
S /cm^2	Active area of working electrode	
F/ C mol^{-1}	Faraday constant	96485 C mol^{-1}
T/K	Thermodynamic temperature	298 K
t_p/s	Time-duration of a potential pulse in SWV	
f/Hz	Frequency of the applied SW pulses	$f = t_p/2$
Γ^*(Ox)/mol cm^{-2}	Initial surface concentration of redox adsorbate Ox	
Γ(Ox), Γ(Red) and Γ(Z) /mol cm^{-2}	Surface concentrations of molecules of Ox, Red, and Z, respectively	
c(Y) /mol cm^{-3}	Molar concentration of the substrate Y dissolved in voltametric cell	
α	Electron transfer coefficient	
R/J mol^{-1}K^{-1}	Universal gas constant	8.314 J mol^{-1}K^{-1}
Φ	Dimensionless potential	$\Phi = \frac{nF}{RT}\left(E - E^{\phi'}\right)$
E / V	Applied potential	
$E^{\phi'}$/ V	Standard (formal) redox potential of redox couple Ox(ads)/Red(ads)	0.00 V
K_{ET}	Dimensionless parameter related to the rate of electron transfer	$K_{ET} = k_s^{\phi}/f$
k_s^{ϕ} / s^{-1}	Standard rate constant of electron transfer	
K_{chem}	Dimensionless parameter related to the rate of irreversible chemical reaction	$K_{chem} = k_c/f$
k_c / s^{-1}	Rate constant of irreversible chemical reaction	$k_c = k_c' \times c$(Y)
k_c'/mol^{-1} cm^3 s^{-1}	Real rate constant of irreversible chemical reaction	
E_{sw} / mV	Amplitude of the square-wave pulses	
dE / mV	Potential increment	4 mV
M	Numerical integration factor	$M = \exp[K_{chem}(m/50)] - \exp[K_{chem}(m\text{-}1)/50]$
m	Serial number of the time intervals in SWV	

Mathematically, the considered mechanism can be described by the following equations:

$$(\mathrm{d}\Gamma(\mathrm{Ox})/\mathrm{d}t) = -I/(nFS) - k_c\Gamma(\mathrm{Ox}) \quad (1)$$

$$(\mathrm{d}\Gamma(\mathrm{Red})/\mathrm{d}t) = I/(nFS) \quad (2)$$

$$(\mathrm{d}\Gamma(\mathrm{Z})/\mathrm{d}t) = k_c\Gamma(\mathrm{Ox}) \quad (3)$$

The differential Eqs. (1 – 3) have been solved under following conditions:

$$t = 0;\ \Gamma(\mathrm{Ox}) = \Gamma^*(\mathrm{Ox});\ \ \Gamma(\mathrm{Red}) = \Gamma(\mathrm{Z}) = 0 \quad (4)$$

$$t > 0;\ \Gamma(\mathrm{Ox}) + \Gamma(\mathrm{Red}) + \Gamma(\mathrm{Z}) = \Gamma^*(\mathrm{Ox}) \quad (5)$$

At the working electrode-electrolyte interface, the Butler-Volmer formalism is assumed to apply (Eq. 6):

$$(I/nFS) = k_s^{\phi}\exp(-\alpha\Phi)\,[\Gamma(\mathrm{Ox}) - \exp(\Phi)\,\Gamma(\mathrm{Red})] \quad (6)$$

To derive a numerical solution for Eq. 6, the methodology reported by Nicholson and Olmstead has been utilized, as outlined in reference.[24] The Supplementary Material accompanying this paper provides the complete MATHCAD file, including

all formulas and parameters necessary for computing the model's dimensionless voltammograms.

Given constant simulation parameters, the primary features of the calculated voltammetric patterns are predominantly governed by two dimensionless parameters: K_{ET} and K_{chem}. The dimensionless kinetic parameter K_{ET} describes the electron transfer step and is defined as:

$$K_{ET} = k_s^{\ominus}/f \quad (7)$$

where $k_s^{\ominus}$ is the standard rate constant of electron transfer, and f is the square-wave frequency. The magnitude of K_{ET} serves as an indicator of the rate of electron transfer occurring between the working electrode and the molecules of adsorbed redox species, Ox and Red, relative to the duration of the applied square-wave pulses.

Conversely, the dimensionless chemical kinetic parameter (K_{chem}) is defined as:

$$K_{chem} = k_c/f \quad (8)$$

where k_c represents the rate constant of the irreversible chemical reaction and f is the frequency of the square-wave pulses. For the mechanism considered, the rate constant k_c in Equation 8 is expressed as:

$$k_c = k_c' \times c(Y) \quad (9)$$

where k_c' denotes the actual chemical rate constant, and c(Y) represents the molar concentration of substrate Y, assumed to be present in excess in the voltammetric cell.

For the computations of theoretical voltammograms discussed in this study, the commercial software package MATHCAD 14 has been employed. In the theoretical model considered, reduction currents are designated as positive, adhering to the US electrochemical convention.

3. RESULTS AND DISCUSSION

3.1. *Description of general voltammetric behavior*

Electrochemical assessment of the oxidation status and the chemical activity of an electrode-confined redox protein is frequently explored as a foundation for theoretical modeling in protein-film voltammetry. The features of theoretical current-potential voltammetric curves often provide insight into the electrode transformation of a given class of redox proteins, while also revealing the kinetic and thermodynamic effects of associated chemical reactions.

Theories of lipophilic redox proteins under cyclic voltammetry and square-wave voltammetry conditions at planar electrodes have already been applied to numerous electrode mechanisms involving coupled chemical reactions. Readers are referred to various works on this topic.[6,11,13,17,20,21,23,25–35] Until now, no theoretical study in square-wave voltammetry has examined a mechanism in which the initial form of a lipophilic redox protein undergoes simultaneously electrochemical transformation and a parallel irreversible chemical inactivation reaction at the working electrode. It is important to note that distinguishing between enzyme irreversible inactivation and film loss under voltammetric conditions is challenging, as both phenomena produce similar effects.[23] This study presents SW voltammetric results that can differentiate between irreversible inactivation and film loss of lipophilic enzyme/protein adsorbed at the working electrode.

This section highlights the key outcomes related to the electrochemical mechanism delineated in Scheme 1, including a detailed discussion on the primary attributes of the computed voltammetric curves, supplemented by illustrative voltammograms to aid in deducing the relevant kinetic parameters. Since this electrochemical mechanism under SWV conditions is a pioneering endeavor, it is essential to represent the voltammetric patterns using two graphical formats: one emphasizing the characteristics of both forward and reverse current components and the other focusing on the net SW voltammograms.

Figures 1a–c show the forward (reduction) and backward (reoxidation) curves of square-wave voltammograms for the considered electrochemical mechanism. The curves in Figure 1 illustrate the effect of the dimensionless chemical parameter K_{chem}, calculated at a moderate rate of electron transfer step (K_{ET} = 1). Curve 1 in Figure 1a was computed under the near absence of chemical reaction, and its attributes correspond to a simple surface electrode mechanism.[26] The influence of chemical rate on the reduction (forward) and oxidation (backward) curves becomes noticeable when $K_{chem} > 0.5$.

Since the irreversible chemical reaction consumes the starting material of the redox protein, an increase in the chemical rate (expressed via K_{chem}) is expected to correspond to a decrease in current intensities of both voltammetric current components. This trend is evident for $K_{chem} > 0.5$ in all patterns shown in Figures 1a–c when $K_{ET} \leq 2.5$. Under such conditions, the effect of chemical reaction rates on the shape of the forward and backward voltammetric curves is an interesting aspect to consider across different K_{chem} regions.

As expected for the current electrochemical mechanism, the currents associated with the reoxidation (backward) voltammetric components decrease as the chemical reaction rate increases. However, the backward current components retain their characteristic peak-like shape across all values of K_{chem}, as seen the reoxidation curves in Figures 1a–c.

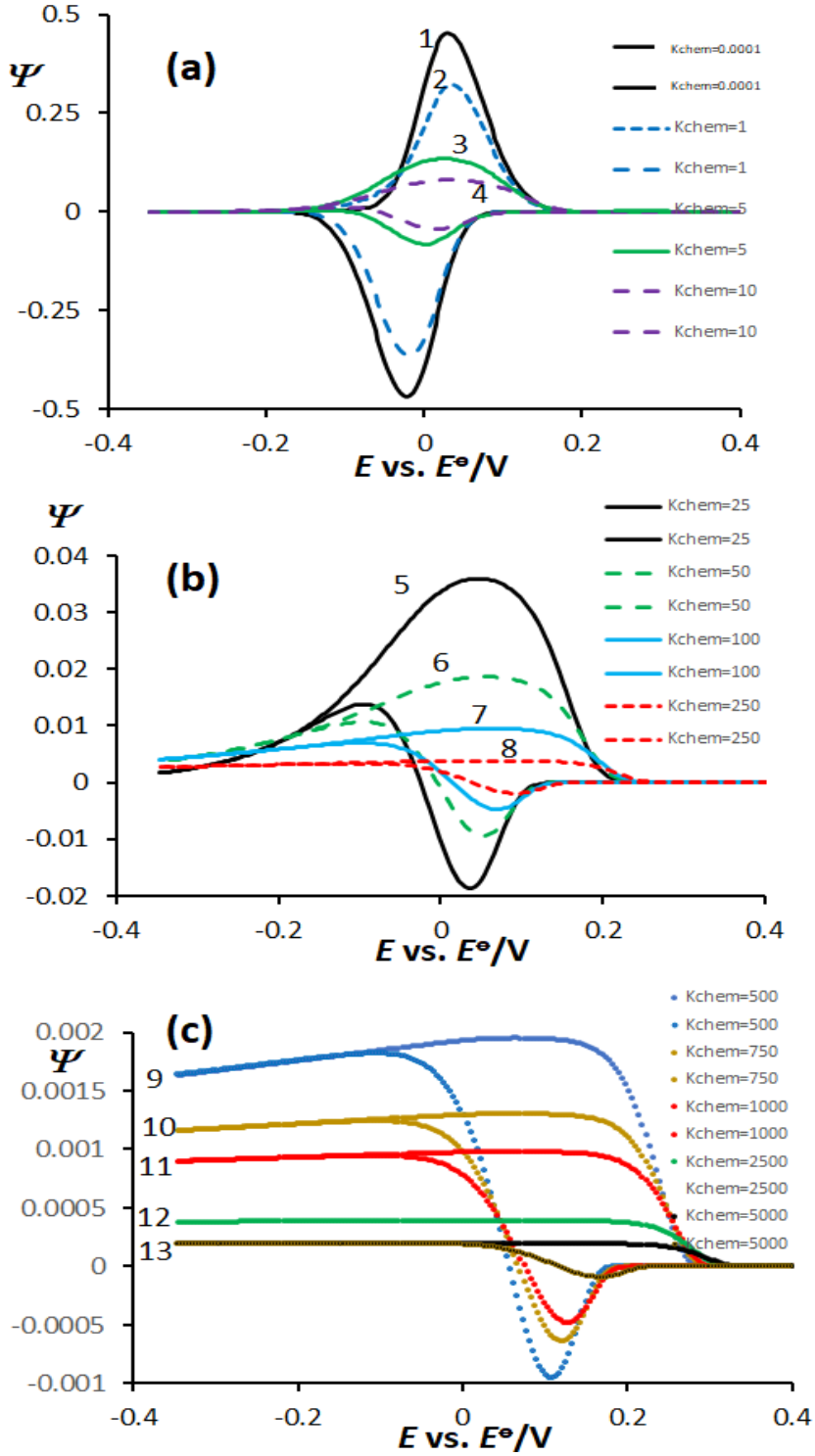

Fig. 1. Effect of dimensionless chemical rate parameter K_{chem} to the features of forward (reduction) and backward (reoxidation) current components of the square-wave voltammograms of considered electrochemical mechanism. Curves are simulated at moderate rate of electron transfer step described with K_{ET} = 1. Other parameters used in calculations are: electron transfer coefficient α = 0.5, number of electrons exchanged n = 1, temperature T = 298 K, square-wave amplitude E_{sw} = 50 mV, potential step dE = 4 mV. Rate of chemical reaction increases in direction from curve 1 on Figure (a) towards curve 13 in Figure (c). The magnitudes of the dimensionless chemical kinetic parameter K_{chem} are given in the patterns. Starting potential in all calculations was set to + 0.4 V.

As K_{chem} increases, not only do the intensities of the currents associated with the forward (reduction) voltammetric curves decrease but significant changes in morphology also occur at high chemical reaction rates. For $5 < K_{chem} < 100$ (curves 3 and 4 in Fig. 1a, and curves 5 and 6 in Fig. 1b), an increase in the chemical reaction rate produces significant broadening of the reduction (forward) curves. These curves eventually adopt a plateau-like shape instead of a peak when $K_{chem} > 200$ (curves 7 and 8 in Fig. 1b and curves 9 – 13 in Fig. 1c).

The distinctive shapes of the reduction voltammetric currents primarily result from the dominance of the chemical reaction rate over the electron transfer rate. Generally, sustained consumption of the initial electroactive material during the current-sampling phase of SW pulses leads to plateau-like reduction current components. For $K_{chem} > 500$, reduction voltammetric current components exhibit plateau-like behavior as the rate of the chemical step increases.

The peculiar shapes of reduction voltammetric currents at higher chemical reaction rates (Fig. 1c) mainly arise from the significant dominance of the chemical reaction rate over the rate of the electron transfer step. This dominance results in a permanent consumption of the initial electroactive material during the current-sampling phase of SW pulses, leading to plateau-like reduction current components. This voltammetric behavior resembles to some aspects patterns in electrochemical-regenerative EC' mechanisms at high regenerative reaction rates.[27]

The unique voltammetric patterns in Figures 1a–c are specific to this electrochemical mechanism and do not resemble patterns associated with protein-film loss[23] or other electrode mechanisms.[26] Consequently, the voltammetric profiles in Figures 1a–c may serve as valuable indicators for identifying this particular electrode mechanism in SWV.

The net SW voltammograms corresponding to the forward-backward curves in Figure 1 are displayed in Figures 2a and b. As expected, the peak currents in net SWV decrease in proportion to the rate of the chemical reaction. At $K_{chem} > 20$, a shoulder-like feature emerges in the ascending branches of net SW voltammograms at positive potentials. The feature originates from the shapes of forward-backward current components (see Fig. 1) observed at $K_{chem} > 20$ and from the definition of net currents in SWV.[26] The net SWV peaks in Figure 2 exhibit another characteristic: shift toward more positive potentials as the chemical step rate decreases in the range of $20 < K_{chem} < 3000$. This behavior is typically linked to electrode mechanisms involving follow-up chemical steps.[34,35] The next section explores this shift in net SWV peaks as a means to construct working curves for determining the rate constant of the chemical step.

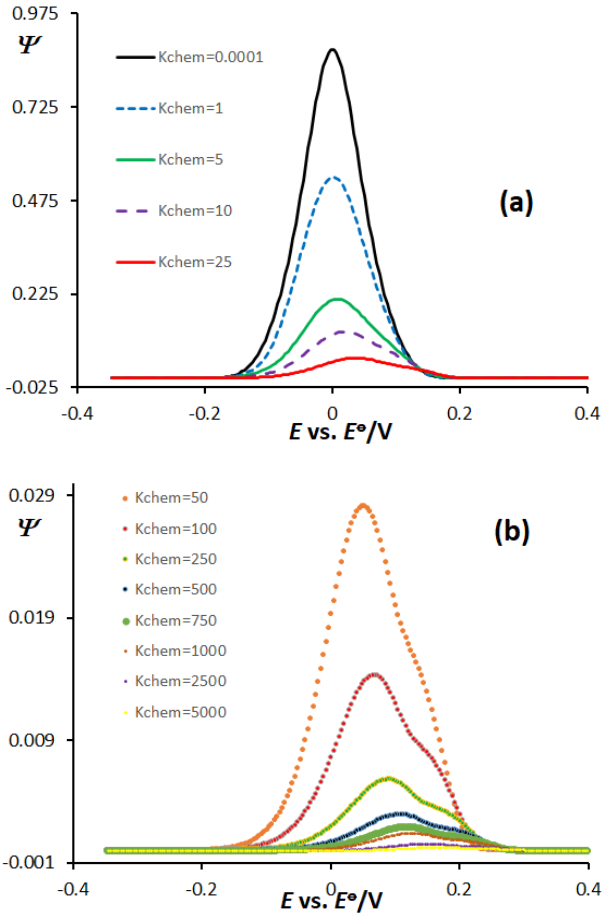

Fig. 2. Effect of dimensionless chemical rate parameter K_{chem} to the characteristics of net square-wave voltammograms of considered electrochemical mechanism, calculated for magnitude of the dimensionless electrode kinetic parameter $K_{ET} = 1$. Rate of chemical reaction increases from top curve in Figure (a) towards curve with lowest current in Figure (b). The magnitudes of the dimensionless chemical kinetic parameter K_{chem} are given in the graphs. Other conditions used in this simulation protocol were same as those reported in Figure 1.

It is worth noting that the mechanism described in this study shares some similarities with film loss in protein-film voltammetry. In protein-film voltammetry, film loss is commonly characterized by a simultaneous decrease in both reduction and oxidation current components as the electrode potential cycles up and down consecutively (particularly when using cyclic voltammetry as a working technique[36]). Figure 3 presents a series of cyclic voltammograms of a surface electrode system illustrating a simple case of film loss after consecutive cycling. The voltammograms in Figure 3 differ significantly from those observed for irreversible inactivation, as shown in the voltammograms in Figure 1.

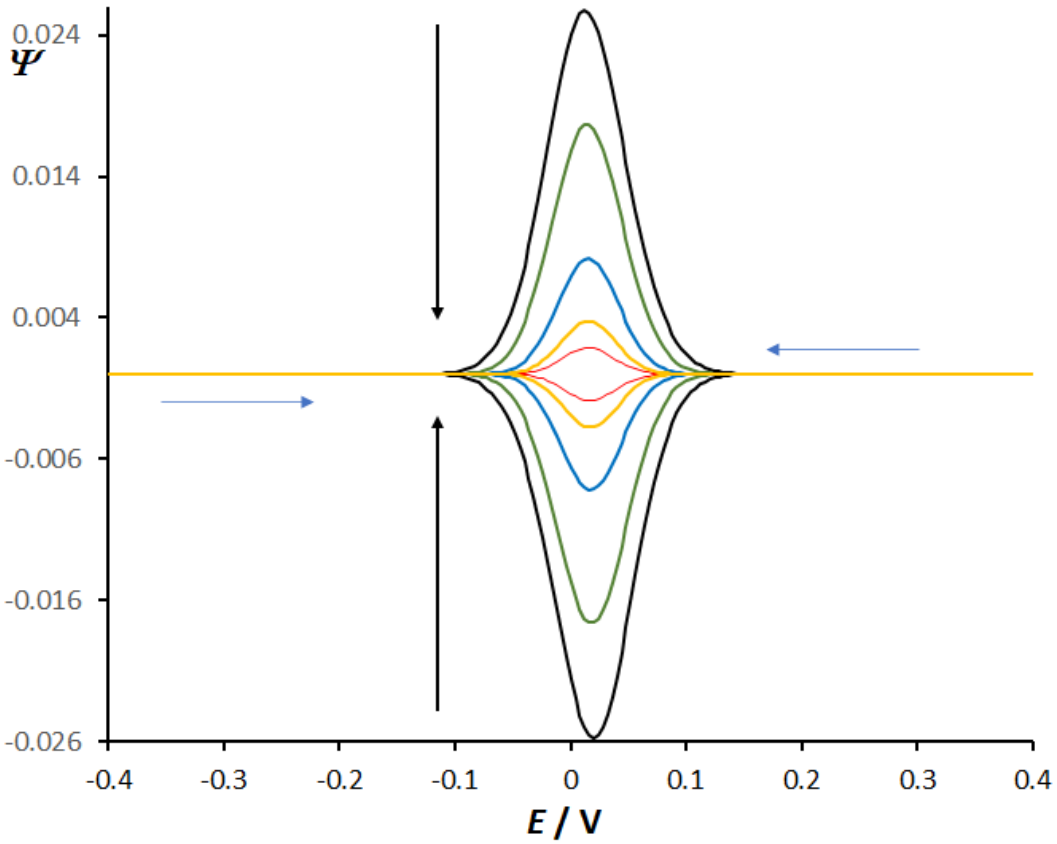

Fig. 3. Cyclic staircase voltammograms simulated for a simple surface electrode mechanism representing the film loss during consecutive scans in protein-film voltammetry. As the number of scans increases, the loss of the film is portrayed in subsequent diminishing of both current components in the directions of the arrows, while the position of both peaks remains unchanged. The protocol used to simulate this set of cyclic voltammograms comprised initial surface concentration of redox adsorbate being only variable. Other simulation conditions were: electron transfer coefficient $\alpha = 0.5$, number of electrons exchanged $n = 1$, temperature $T = 298$ K, potential step d$E = 4$ mV, time duration of potential pulses $\tau = 0.02$ s. Starting potential was +0.4 V, while the switch potential was set to -0.4 V.

When the rate of electron transfer is relatively high, a series of distinctive phenomena emerge in the calculated voltammograms at varying chemical reaction rates. Figures 4a–c illustrates the effect of K_{chem} on the voltammetric curves of reduction (forward) and reoxidation (backward) current components. All voltammetric curves in Figure 4 are simulated at a relatively high electron transfer rate ($K_{ET} = 10$). In general, increasing the rate of the chemical step within the range $0.5 < K_{chem} < 5$ leads to a significant decrease in the peak-to-peak separation between forward and backward peaks. More intriguingly, within this same range of chemical rates ($0.5 < K_{chem} < 5$), both reduction and reoxidation current components increase, instead of decrease, as K_{chem} increases. For instance, the peak current of the reduction component rises approximately fourfold, while the reoxidation component increases by about twofold as K_{chem} increases from 0.1 to 5.0 (compare curve 1 and curve 5 in Fig. 4a). Similar phenomena have been observed in surface electrode mechanisms coupled with follow-up chemical reactions; readers can find detailed explanations elsewhere.[34,35]

In Figure 4a, the behavior of the voltammetric curves can be explained by considering the characteristics of surface electrochemical reactions with very fast electron transfer rates. In such cases, voltammograms typically exhibit small detected currents due to the rapid conversion of most Ox(ads) species into Red(ads) during the dead-time of applied potential pulses.[26,30] Since SWV samples the current at the end of each SW pulses, only a small fraction of initial redox form Ox(ads) remains available for electrochemical conversion at the end of the pulse (curve 1 in Fig. 4a). However, if Ox(ads) participates in a parallel chemical reaction, the chemical reaction rate can disrupt the equilibrium of the electrochemical step [Ox(ads) + $ne^- \leftrightarrow$ Red(ads)] established during the dead-time of potential pulses. This results in a greater fraction of Ox(ads) remaining available for redox transformation at the working electrode surface when current is being sampled in SWV.[26,35] Consequently,

all SWV current components increase within the region of moderate chemical step rates, as displayed in the voltammograms in Figure 4a.

Eventually, for chemical step rates characterized by K_{chem} > 5 (curves 6 – 10 in Fig. 4b and curves 11 – 15 in Fig. 4c), both reduction and reoxidation current components decrease as K_{chem} increases. In this range of chemical reaction rates (K_{chem} > 5), voltammetric behavior similar to that illustrated in Fig. 1 is observed. The apparent plateau condition of the forward (reduction) current components becomes pronounced at chemical rates exceeding K_{chem} > 500 (see the curves in Fig. 4e).

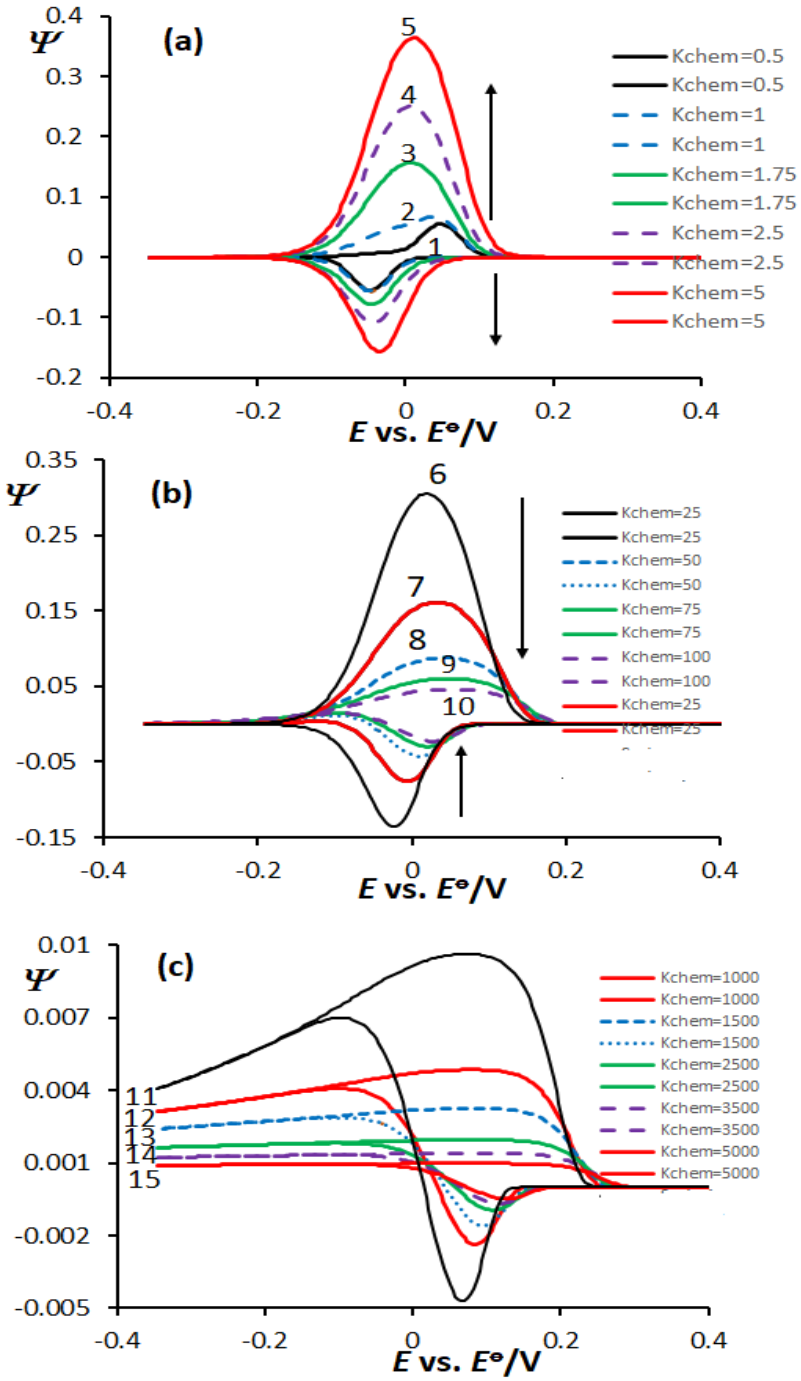

Fig. 4. Effect of dimensionless chemical rate parameter K_{chem} to the attributes of forward (reduction) and backward (reoxidation) current components of the square-wave voltammograms of considered electrochemical mechanism, simulated at fast rate of electron transfer step for K_{ET} = 10. Rate of chemical reaction increases from curve 1 on Figure (a) towards curve 15 in Figure (c). The magnitudes of the dimensionless chemical kinetic parameter K_{chem} are given in the graphs. Other conditions used in this simulation protocol were identical as those in Figure 1.

When discussing net SW voltammograms under these conditions, it is important to highlight the splitting of the net SWV peak,[26,30] a characteristic feature of all surface-confined electrode mechanisms with high electron transfer rates (see curve 1 in Fig. 5a). Increasing the rate of the chemical reaction in the range $0.5 < K_{chem} < 5$ leads to the disappearance of the splitting phenomenon of the SWV peaks (curves 3 – 5 in Fig. 5a). Additionally, within this same range of rates of chemical step ($0.5 < K_{chem} < 5$), a significant increase in the net SWV peak currents occurs as K_{chem} increases.

The expected decrease in the net SWV peak currents becomes evident when $K_{chem} > 5$ (curves 6 – 10 in Fig. 5b, and curves 11 – 15 in Fig. 5c). In this region of chemical reaction rates, a shoulder-like feature appears on the ascending branches of the net SWV peaks calculated for $K_{chem} > 50$. As with previous cases discussed in this work, when chemical reaction rates fall within the range $25 < K_{chem} < 5000$, the positions of the net SWV peaks shifts to more positive potentials.

Indeed, the features of the voltammetric curves in Figures 4 and 5 can serve as useful tools for identifying this mechanism, which is characterized by a high rate of the electron transfer step.

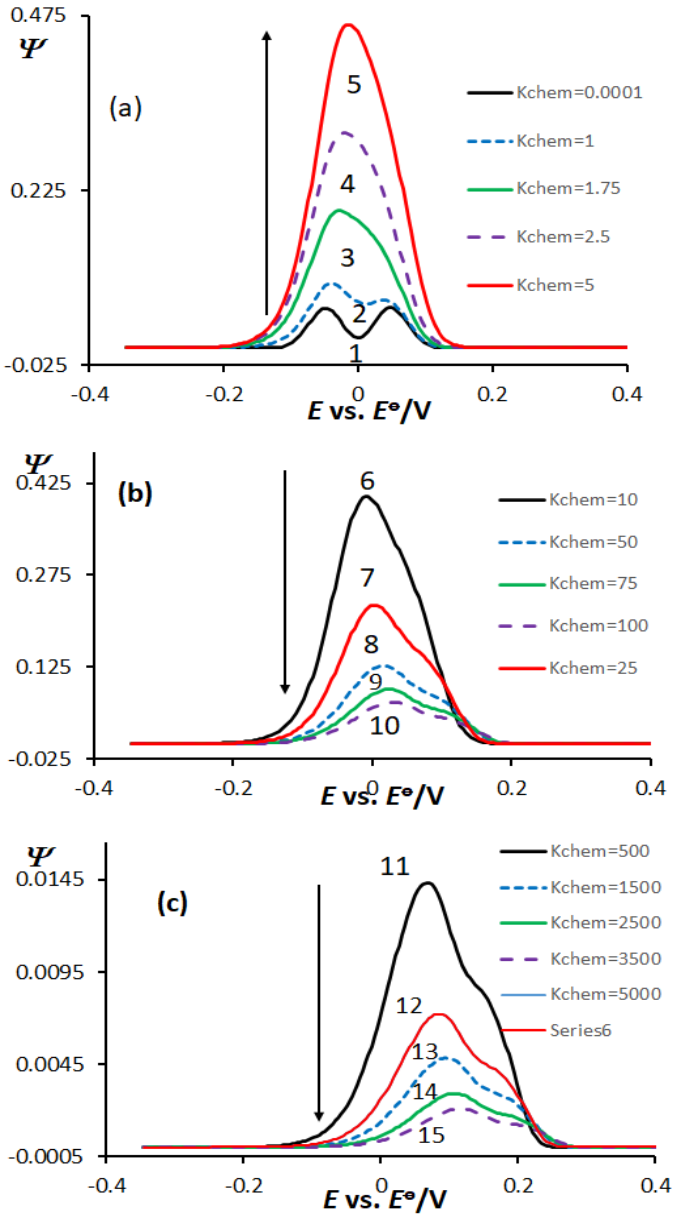

Fig. 5. Effect of dimensionless chemical rate parameter K_{chem} to the features of net square-wave voltammograms of considered electrochemical mechanism, calculated for magnitude of the dimensionless electrode kinetic parameter $K_{ET} = 10$. Rate of chemical reaction increases from curve 1 in Figure (a) towards curve 15 in Figure (c). The magnitudes of the dimensionless chemical kinetic parameter K_{chem} are given in the graphs. Other conditions used in this simulation protocol were identical as those in Figure 1.

3.2. *Clues to accessing the kinetic parameters relevant to the electrode mechanism*

Upon determining the characteristics of the electrode mechanism discussed in this study, the next step was to ascertain the physical parameters associated with the electron transfer process ($k_s^{\ominus}$, α) and the chemical reaction (k_c).

In addition to the phenomenon of splitting of the net SWV peak, as displayed in curve 1 of Fig. 5a,[26,30] another useful approach for determining the standard rate constant of the electron transfer step ($k_s^{\ominus}$) is the feature known as the quasireversible maximum.[26] This effect is commonly observed in all surface-confined electrode mechanisms, where net SWV peak currents exhibit a parabolic dependence on the applied SW frequency. This phenomenon arises from the interplay between the specific chronoamperometric properties of the surface electrode reaction and the current sampling procedure used in SWV. Further explanations of its causes of can be found in the work.[26]

Generally, the synchronization of the electron exchange rate between the working electrode and the redox adsorbates using the current measuring frequency in SWV leads to recycling of electrochemically active material within the timeframe of SW pulses. As a result, electrochemical systems with moderate rates of electron transfer exhibit significantly higher measured currents compared to those with fast electron transfer rates. By experimentally observing the quasireversible maximum, one can determine the standard rate constant of electron transfer ($k_s^{\ominus}$) using the provided protocols outlined in the work.[26]

Figure 6 presents a series of quasireversible maxima constructed as a function of the chemical step rate. As reported in the work,[26] the position of the quasireversible maximum is closely related to the apparent reversibility of the electrode reaction. Therefore, two key conclusions can be drawn from Fig. 6: 1) for low chemical step rates (up to K_{chem} = 0.1), the position of the quasireversible maximum is independent of K_{chem}; 2) for higher chemical step rates (K_{chem} > 0.25), the position of the quasireversible maximum depends on K_{chem}, shifting toward higher K_{ET} values as the chemical step rate increases (curves 3 – 5 in Fig. 6).

Curves 1 and 2 in Figure 6 suggest that the quasireversible maximum feature could potentially be used to determine $k_s^{\ominus}$, following the procedure described elsewhere,[26] but only when measured at the low chemical step rates of the electrode mechanism. However, in real experimental scenarios, the curves in Fig. 6 can be reproduced by varying the SW frequency. Since the SW frequency simultaneously affects both dimensionless parameters (K_{ET} and K_{chem}), such an analysis may lead to erroneous results. A more reliable approach for determining the magnitude of $k_s^{\ominus}$ is to explore the approach of splitting the net SWV peak under the influence of square-wave amplitude.[26] Alternatively, this amplitude-based quasireversible maximum approach,[37] along with other methods,[38,39] may also be employed. To determine the electron transfer parameter (α), one can use the methodology outlined in the work.[40]

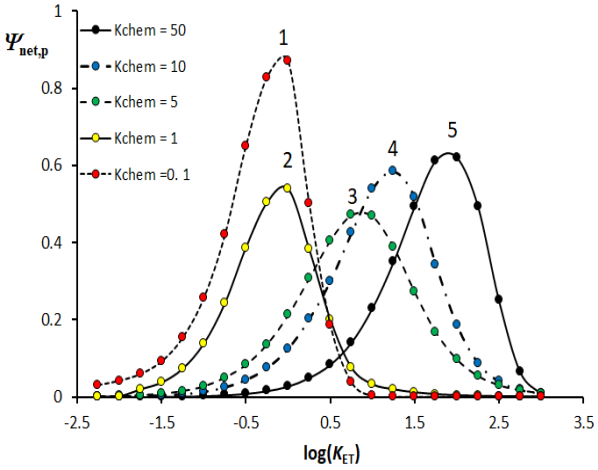

Fig. 6. A series of "quasireversible maxima" constructed for several different rates of the chemical reaction. The magnitudes of the dimensionless chemical kinetic parameter K_{chem} used for constructing of every single "quasireversible maximum" are given in the graph. Other conditions used in this simulation protocol were identical as those in Figure 1.

One of the defining characteristics of electrode mechanism is the shift in net SWV peak positions toward more positive potentials as the rate of the chemical step increases (see net SWV peaks in Figs. 2 and 5). Figure 7 illustrates the relationship between net SWV peak potentials ($E_{net,p}$) and log(K_{chem}). The curves in Figure 7 are estimated for three different values of K_{ET}. In all working curves presented in Figure 7, a largely sigmoidal dependences exists between $E_{net,p}$ and log(K_{chem}), with linear sections mostly observed in the 0.5 < log(K_{chem}) < 3.0 region. Within this range of chemical reaction rates, a linear dependence exists between $E_{net,p}$ and log(K_{chem}), with nearly identical slopes of the linear lines close to +59 mV.

The equations describing the linear portions of the curves in Figure 6 are as follows: for K_{ET} = 5: $E_{net,p}$ /V = 0.059 log(K_{chem}) – 0.081 V; for K_{ET} = 1: $E_{net,p}$/V = 0.058 log(K_{chem}) – 0.0372 V; and for K_{ET} = 0.056$E_{net,p}$ /V = 0.058 log(K_{chem}) + 0.0323 V.

These equations, corresponding to the linear segments of the $E_{net,p}$ vs. log(K_{chem}) dependences in Figure 7, can be used to determine the rate of the chemical reaction, provided that the magnitude of K_{ET} has been previously determined.

When conducting experiments on systems known to follow this electrode mechanism, it is crucial to control the introduction of substrate Y into the electrochemical cell with the initiation of voltammetric scans. This synchronization is essential because the chemical reaction within this electrochemical mechanism can proceed even in the absence of an applied potential.

Using a conventional electrochemical cell can present challenges in aligning the onset of chemical reaction inactivation with the initiation of voltage bias, particularly for systems with rapid chemical reaction rates. One potential solution to this issue is the use of flow-through voltammetric cells.[41,42]

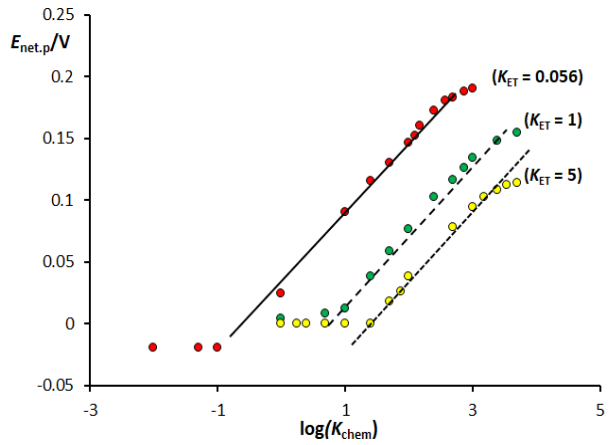

Fig. 7. Working curves presenting net SW peak potentials ($E_{net,p}$) as a function of log(K_{chem}), calculated at three different kinetics of electron transfer step. The values of K_{ET} used in this set of simulations are given in the graph. Other conditions used in simulations were identical as in Figure 1.

4. CONCLUSIONS

While significant advancements have been made in theoretical research on protein-film voltammetry (PFV) over the past two decades, several challenges remain in voltammetric data interpretation. For example, when conducting experiments with lipophilic proteins under voltammetric conditions, differentiating between the irreversible inactivation of the initial form of a redox protein and the loss of the protein film from the working electrode presents a considerable challenge.[36] Irreversible inactivation processes frequently occur in PFV experiments.[23]

The comprehensive review[23] details: anaerobic inactivation of Ni-Fe hydrogenases; nitrate reductase inactivation in the presence of excess of nitrates; bilirubin oxidase and multi-copper oxidase inactivation triggered by chlorides; horseradish peroxidase inactivation due to high concentrations of hydrogen peroxide; and oxidative inactivation of FeFe hydrogenases. These reductions are just a few examples of common inactivation reactions studied in PFV.

This work presents a comprehensive set of theoretical findings on the voltammetric characteristics of lipophilic redox enzymes and other surface-active systems. The initial form of these lipophilic surface-active chemical systems undergoes an electrode transformation and a simultaneous irreversible chemical change, known as irreversible inactivation. By analyzing this model under square-wave voltammetry conditions, readers gain access to a wide array of voltammetric curves that contribute to a deeper understanding and characterization of this important electrochemical mechanism.

Table 2 provides a systematic review of the reduction and oxidation curves associated with this mechanism, analyzed in relation to the electron transfer rate and the rate of the irreversible chemical reaction. The voltammetric curves presented in Table 2 are characteristic of this particular electrochemical mechanism, enabling a clear differentiation between this mechanism and protein-film loss, as well as other systems involving preceding, regenerative, or subsequent chemical reactions.

Furthermore, by referencing insights from the previous section 3, researchers can identify the appropriate voltammetric methodology to determine all relevant physical parameters associated with this mechanism. The initial findings presented here aim to establish a solid foundation for developing novel protocols related to the inhabitation/inactivation processes of lipophilic redox proteins under square-wave protein-film voltammetry conditions.

At this stage, it is important to note that time-based (or frequency-based) analysis in square-wave voltammetry is not a reliable method for extracting kinetic parameters associated with this mechanism. This limitation arises because a time-based analysis simultaneously affects both the kinetic parameter related to the electron transfer step (K_{ET}) and the dimensionless parameter associated with the kinetics of the chemical step (K_{chem}). Therefore, due to the mechanistic features discussed in this study, applying time- or frequency-based analysis may lead to erroneous or misleading interpretations.

T a b l e 2

Reduction (forward) and reoxidation (backward) components of the square-wave voltammetric patterns were calculated at different rates of electron transfer step and different kinetics of the irreversible chemical reaction. For the voltammograms display, a square-wave amplitude of 80 mV and a potential step of 4 mV were used. The electron transfer coefficient in all simulations was set to $\alpha = 0.5$. The starting potential was set to +0.4 V.

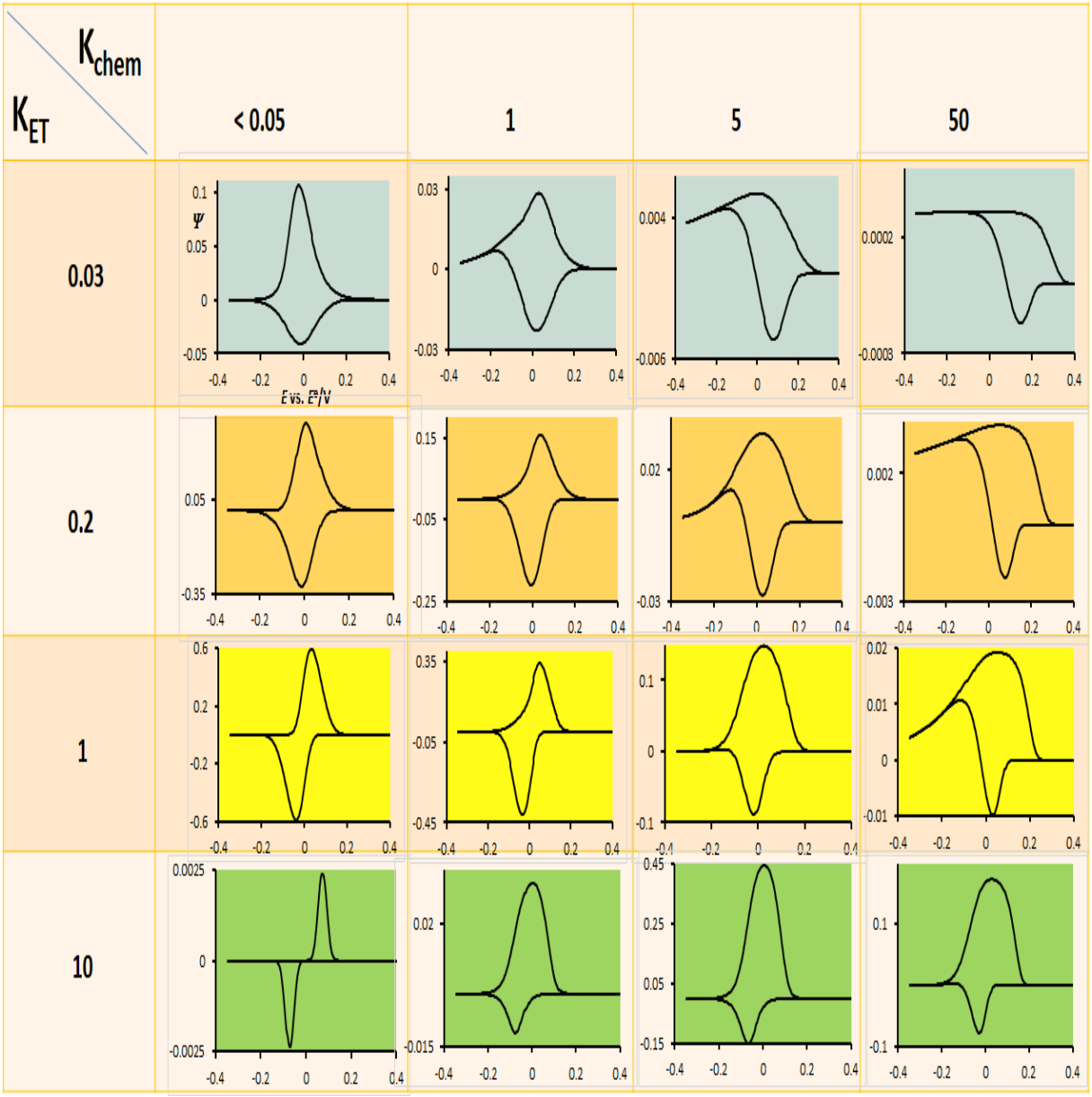

REFERENCES

(1) El Harrad, L., Bourais, I., Mohammadi, H., Amine, A., Recent advances in electrochemical biosensors based on enzyme inhibition for clinical and pharmaceutical applications, *Sensors* **2018**, *18*, 164. doi:10.3390/s18010164

(2) Leger, C., Bertrand, P., Direct electrochemistry of redox enzymes as a tool for mechanistic studies, *Chem. Rev.* **2008**, *108*, 2379–2438. https://doi.org/10.1021/cr0680742

(3) Armstrong, F. A., Electrifying metalloenzymes. In: Cho, A. E., Goddard III, W. A., Eds.; *Metalloproteins: Theory, Calculations and Experiments*, CRC Press, Taylor & Francis Group, London, New York, 2015.

(4) Armstrong, F. A., Applications of voltammetric methods for probing the chemistry of redox proteins. In: Lenaz, G., Milazz, G., Eds., *Bioelectrochemistry: Principles and Practice*, Birkhäuser Verlag AG, Basel, 1997.

(5) Jenner, L. P., Butt, J. N., Electrochemistry of surface-confined enzymes: Inspiration, insight, and opportunity

for sustainable biotechnology, *Curr. Opin. Electrochem*. **2018**, *8*, 81–88. https://doi.org/10.1016/j.coelec.2018.03.021

(6) Kano, K., *Biosci. Biotechnol. Biochem*. **2022**, *86*, 141-156. https://doi.org/10.1093/bbb/zbab197

(7) Fourmond, V., Leger, C., An introduction to electrochemical methods for the functional analysis of metalloproteins, in: Crichton, R. R., Louro, R. O., Eds.; *Practical Approaches to Biological Inorganic Chemistry*, Elsevier, **2020**, pp. 325.

(8) Gulaboski, R., Mirceski, V., Bogeski, I., Hoth, M., Protein film voltammetry-electrochemical enzymatic spectroscopy. A review on recent progress. *J. Solid State Electrochem*. **2012**, *16*, 2315–2328. https://doi.org/10.1007/s10008-011-1397-5

(9) Hirst, J., Direct measurement by protein-film voltammetry, *Biochim. Biophys. Acta Bioenerg*. **2006**, *1757*, 225–239. https://doi.org/10.1016/j.bbabio.2006.04.002.

(10) Gulaboski, R., Kokoskarova, P., Mitrev, S., Theoretical aspects of several successive two-step redox mechanisms in protein-film cyclic staircase voltammetry, *Electrochim. Acta* **2012**, *69*, 86–96. DOI: 10.1016/j.electacta.2012.02.086

(11) Lopez-Tenes, M., Gonzalez, J., Molina, A., Two electron transfer reactions in electrochemistry for solution-soluble and surface-confined molecules: A common approach, *J. Phys. Chem. C* **2014**, *118*, 12312–12324. DOI:10.1021/jp5025763

(12) Zhang, H. N., Guo, Z. Y., Gai, P. P., Research progress in protein film voltammetry, *Chin. J. Anal. Chem*. **2009**, *37*, 461–465. https://doi.org/10.1016/S1872-2040(08)60093-6

(13) Gonzalez, J., Lopez-Tenes, M., Molina, A., Voltammetry of electrochemically reversible systems at electrodes at any geometry: A general, explicit, analytical characterization, *J. Phys. Chem. C* **2013**, *117*, 5208–5220. https://doi.org/10.1021/jp109587b

(14) Mann, M. A., Bottomley, L. A., Cyclic square-wave voltammetry of surface-confined quasireversible electron transfer reactions, *Langmuir* **2015**, *31*, 9511–9520. https://doi.org/10.1021/acs.langmuir.5b01684

(15) Stevenson, G. P.; Lee, C.-Y.; Kennedy, G. F.; Parkin, A.; Baker, R. E.; Gillow, K.; Armstrong, F. A.; Gavaghan, D. J.; Bond, A. M., Theoretical analysis of the two-electron transfer reaction and experimental studies with surface-confined cytochrome c peroxidase using large-amplitude Fourier transformed AC voltammetry. *Langmuir* **2012**, *28*, 9864– 9877. DOI: 10.1021/la205037e

(16) Fourmond, V., Wiedner, E. S., Shaw, W. J., Léger, C., Understanding and design of bidirectional and reversible catalysts of multielectron, multistep reactions, *J. Am. Chem. Soc*. **2019**, *141*, 11269–11285. https://doi.org/10.1021/jacs.9b04854

(17) Gonzalez, J., Sequí, J.-A., Analysis of the electrochemical response of surface-confined bidirectional molecular electrocatalysts in the presence of intermolecular interactions, *ChemCatChem*. **2021**, *13*, 747–762. https://doi.org/10.1002/cctc.202001599

(18) Mirceski, V., Guziejewski, D., Gulaboski, R. Differential square-wave voltammetry, *Anal. Chem*. **2019**, *91*, 14904–14910. DOI: 10.1021/acs.analchem.9b03035

(19) Léger, C., Elliott, S. J., Hoke, K. R., Jeuken, L. J. C., Jones, A. K., Armstrong, F. A., Enzyme electrokinetics: using protein film voltammetry to investigate redox enzymes and their mechanisms, *Biochemistry* **2003**, *42*, 8653–8662. https://doi.org/10.1021/bi034789c

(20) Gulaboski, R., Mirceski, V., Lovric, M., Critical aspects in exploring time analysis for the voltammetric estimation of kinetic parameters of surface electrode mechanisms coupled with chemical reactions, *Maced. J. Chem. Chem. Eng*. **2021**, *40*, 1–9. https://doi.org/10.20450/mjcce.2021.2270

(21) Janeva, M., Kokoskarova, P., Maksimova, V., Gulaboski, R., Square-wave voltammetry of two-step surface electrode mechanisms coupled with chemical reactions – A theoretical overview, *Electroanalysis* **2019**, *31*, 2488–2506. https://doi.org/10.1002/elan.201900416

(22) Gulaboski, R., Mirceski, V., Application of voltammetry in biomedicine – Recent achievements in enzymatic voltammetry. *Maced. J. Chem. Chem. Eng*. **2020**, *39*, 153–166. https://doi.org/10.20450/mjcce.2020.2152

(23) Del Barrio, M., Fourmond, V., Redox (in)activation of metalloenzymes: A protein film voltammetry approach, *ChemElectroChem*. **2019**, *6*, 4949–4962. https://doi.org/10.1002/celc.201901028

(24) Olmstead, M. L., Hamilton, R. G., Nicholson, R. S., Theory of cyclic voltammetry for a dimerization reaction initiated electrochemically, *Anal. Chem*. **1969**, *41*, 260–267. https://doi.org/10.1021/ac60271a032

(25) Molina, A., González, J., *Pulse Voltammetry in Physical Electrochemistry and Electroanalysis*. In: Scholz, F., Ed., *Monographs in Electrochemistry*, Springer, Berlin Heidelberg, **2016**.

(26) Mirceski, V., Komorsky-Lovric, S., Lovric, M., *Square-Wave Voltammetry: Theory and Application*. Scholz, F., Ed., Springer, Berlin, Heidelberg, **2007**.

(27) Gulaboski, R., Mirceski, V., New aspects of electrochemical-catalytic (EC') mechanism in square-wave voltammetry, *Electrochim. Acta* **2015**, *167*, 219–225. https://doi.org/10.1016/j.electacta.2015.03.175

(28) Mirceski, V., Gulaboski, R., Surface catalytic mechanism in square-wave voltammetry, *Electroanalysis* **2001**, *13*, 1326–1334. https://doi.org/10.1002/1521-4109(200111)13:16<1326::AID-ELAN1326>3.0.CO;2-S

(29) Waskasi, M. M., Martin, D. R., Matyushov, D. V., Wetting of the protein active site leads to non-Marcusian reaction kinetics, *J. Phys. Chem. B* **2018**, *122*, 10490-10495. DOI: 10.1021/acs.jpcb.8b10376

(30) Mirčeski, V., Lovrić, M., Split square-wave voltammograms of surface redox reactions, *Electroanalysis* **1997**, *9*, 1283–1287. https://doi.org/10.1002/elan.1140091613

(31) Blumberger, J., Recent advances in theory and molecular simulation of biological electron transfer reactions, *Chem. Rev*. **2015**, *115*, 11191–11238. https://doi.org/10.1021/acs.chemrev.5b00298

(32) Gulaboski, R., Mirčeski, V., Lovrić, M., Bogeski, I., Theoretical study of a surface electrode reaction preced-

ed by a homogeneous chemical reaction under conditions of square-wave voltammetry, *Electrochem. Commun*. **2005**, *7*, 515-522. https://doi.org/10.1016/j.elecom.2005.03.009

(33) Mirčeski, V., Lovrić, M., Gulaboski, R., Theoretical and experimental study of the surface redox reaction involving interactions between the adsorbed particles under conditions of square-wave voltammetry, *J. Electroanal. Chem*. **2001**, *515*, 91–100.

(34) Gulaboski, R., Theoretical contribution towards understanding specific behavior of "simple" protein-film reactions in square-wave voltammetry, *Electroanalysis* **2019**, *31*, 545–553. DOI:10.1002/elan.201800739

(35) Gulaboski, R., Janeva, M., Maksimova, V., New aspects of protein-film voltammetry of redox enzymes coupled to follow up reversible chemical reaction in square-wave voltammetry, *Electroanalysis* **2019**, *31*, 946–956. https://doi.org/10.1002/elan.201900028

(36) Gulaboski, R., Distinction between film loss and enzyme inactivation in protein-film voltammetry: a theoretical study in cyclic staircase voltammetry, *Monatsh. Chem.* **2023**, *154*, 141–149. DOI: 10.1007/s00706-022-02999-5

(37) Guziejewski, D., Mirceski, V., Jadresko, D., Measuring the electrode kinetics of surface confined electrode reactions at constant scan rate, *Electroanalysis* **2015**, *27*, 67–73. https://doi.org/10.1002/elan.201400349

(38) Jadreško, D., Guziejewski, D., Mirčeski, V., Electrochemical Faradaic spectroscopy, *ChemElectroChem.* **2018**, *5*, 187–194. https://doi.org/10.1002/celc.201700784

(39) Mirceski, V., Laborda, E., Guziejewski, D.; Compton, R. G. New approach to electrode kinetic measurements in square-wave voltammetry: Amplitude-based quasi-reversible maximum, *Anal. Chem*. **2013**, *85*, 5586–5594. https://doi.org/10.1021/ac4008573

(40) Gulaboski, R., Lovrić, M., Mirceski, V., Bogeski, I. Hoth, M., A new rapid and simple method to determine the kinetics of electrode reactions of biologically relevant compounds from the half-peak width of the square-wave voltammograms, *Biophys. Chem*. **2008**, *138*, 130–137. http://hdl.handle.net/20.500.12188/13892

(41) Rial-Rodriguez, E., Williams, J. D., Eggenweiler, H-M., Fuchss, T., Sommer, A., Kappe, C. O., Cantillo, D., Development of an open-source flow-through cyclic voltammetry cell for real-time inline reaction analytics, *Reac. Chem. Eng*. **2024**, *9*, 26–30. https://doi.org/10.1039/D3RE00535F

(42) Gunasingham, H.; Fleet, B., Hydrodynamic voltammetry in continuous-flow analysis. In: *Electroanalytical Chemistry:* A series of advances, Vol. 16, Marcel Dekker, New York, **1990**, pp. 89–180.

(43) Butt, J. N., Jeuken, L. J. C., Zhang, C., Burton, J. A. J., Sutton-Cook, A. L., Protein film electrochemistry, *Nat. Rev. Methods Primers*, **2023**, *3*. https://doi.org/10.1038/s43586-023-00271-6